Energetic substrate availability regulates synchronous activity in an excitatory neural network

David S. Tourigny[a,b,1,2], Muhammad Kaiser Abdul Karim[c], Rodrigo Echeveste[d], Mark R. N. Kotter[c,2], John S. O'Neill[a,2]

[a] MRC Laboratory of Molecular Biology, Cambridge Biomedical Campus, Francis Crick Ave, Cambridge CB2 0QH, UK
[b] Columbia University Medical Center, 630 W 168th St, New York, NY 10032, USA
[c] Department of Clinical Neurosciences and Wellcome Trust- MRC Cambridge Stem Cell Institute, University of Cambridge, Cambridge Biomedical Campus, Forvie Site, Robinson Way, Cambridge CB2 0SZ, UK
[d] Computational and Biological Learning Lab, Department of Engineering, University of Cambridge, Trumpington Street, Cambridge CB2 1PZ, UK
[1] Lead contact
[2] Correspondence: dst2156@cumc.columbia.edu (DST); mrk25@cam.ac.uk (MRNK); oneillj@mrc-lmb.cam.ac.uk (JSO)

Abstract

Neural networks are required to meet significant metabolic demands associated with performing sophisticated computational tasks in the brain. The necessity for efficient transmission of information imposes stringent constraints on the metabolic pathways that can be used for energy generation at the synapse, and energetic substrate availability has been shown to reduce the efficacy of synaptic function. Here we take a combined experimental-computational approach to study the effects of energetic substrate availability on global neural network behavior and find that glucose alone can sustain excitatory neurotransmission required to generate high-frequency synchronous bursting that emerges in culture. In contrast, obligatory oxidative energetic substrates such as lactate and pyruvate are unable to substitute for glucose, indicating that glycolysis is the primary metabolic pathway underlying coordinated network activity. Our experimental results and computational modelling therefore support recent suggestions that glycolysis serves as the predominant source of ATP for synaptic vesicle recycling at presynaptic nerve terminals.

Significance Statement

The metabolic demands of neurons in the waking human brain are extremely high, accounting for almost a quarter of the body's overall ATP turnover, and therefore precise regulation of neuronal metabolism is essential for energy-efficient encoding of information in the cortex. Using multi-electrode arrays we show that excitatory human cortical neuronal cultures,

directly-derived from ES cells, develop synchronised network behaviour as they mature over several weeks. We use this robust and reproducible platform to understand the metabolic underpinnings of neuronal networks. Exploiting a combined experimental-computational model of metabolic regulation, we provide evidence that glycolytic ATP production is required to sustain the high rates of synaptic vesicle turnover that are essential for coordinated network behaviour.

Introduction

Accurately processing, storing, and retrieving information comes at a considerable metabolic cost to the central nervous system (1). It is currently thought that the human brain is responsible for 20% of all energy consumed by the body, whilst comprising only 2% of the total body weight (2). The energy required to sustain cortical signaling has been estimated (3, 4), and mechanisms mediating synaptic transmission (including glutamate accumulation in vesicles) are predicted to monopolize 41% of all ATP turnover in the cortex (5). Theoretical considerations suggest that cortical networks therefore maximize the ratio of information transmitted to energy consumed (6), which could explain why the mean firing rate of neurons is much lower than that predicted to maximize total coding capacity (3, 7). Mathematical models of energy-efficient neurotransmission also lead to the surprising conclusion that synaptic vesicle release probability is low and synaptic failures should occur often (5, 8). Additional factors thought to minimize energy consumption include economic network wiring constraints (9), but even with these adaptations the metabolic cost of cortical function remains a large proportion of a neuron's energy budget.

To meet this energetic demand, the cortex has evolved an extensive neurovascular coupling that can increase blood flow to regions of high activity. Astrocytes and other glial cells in contact with blood vessels are important regulators of brain energy supply and play a key role providing neurons with a readily accessible fuel source (10, 11). The nature of this neuron-astrocyte relationship remains controversial however, with conflicting theories concerning the primary substrate of resting *versus* active neural metabolism as well as the relative fluxes through metabolic pathways in the two cell types (12-14). Hemodynamic signals based on blood-oxygen-level-dependent functional magnetic resonance-based imaging (BOLD fMRI) show that oxygen uptake during neural activity is disproportionally small compared to that

required for complete oxidation of glucose (i.e. $6O_2$ per glucose consumed), suggesting that glycolysis is the major metabolic pathway of active cortex (15). This observation led to a proposal that neural activity induces aerobic glycolysis in astrocytes, which then produce lactate to serve as the main fuel source for neurons (16, 17). Whilst, as an energetic substrate, lactate can support some aspects of synaptic function (18, 19), the astrocyte-neuron lactate shuttle hypothesis challenges the long-standing consensus that glucose is the principal fuel source of neuronal metabolism (13). Recent studies still support the idea that significant amounts of glucose feed directly into neuronal glycolysis however (e.g. (20-22)), and advancements in fluorescent imaging demonstrate that activity stimulates glycolysis, but not lactate uptake (23).

Presynaptic nerve terminals are unusual in the sense that the majority lack mitochondria but are able to satisfy the sizable ATP-consumption requirements of synaptic vesicle recycling (24, 25). ATP production must be able to increase rapidly in order to meet acute changes in presynaptic demands, and so it is perhaps not surprising that recent work has highlighted the importance of locally-derived glycolytic ATP generation and glucose transport in the synaptic vesicle cycle (26, 27). Neuronal activity has been associated with localization of key glycolytic enzymes to the presynaptic terminal (28), and several of these proteins are enriched in synaptic vesicles (29, 30) where they are found to be essential for synaptic vesicle re-acidification and glutamate uptake (31, 32). Vesicle recycling is a highly dynamic and energetically-demanding process (33, 34) for which ATP supply *via* glucose oxidation alone is presumably too slow (35, 36). Consequently, metabolic stress induced at individual excitatory presynapses by substrate depletion has been shown to reduce the number of functional release sites and depress rates of synaptic vesicle recovery (37, 38). It is not yet understood, however, whether these changes in central carbon metabolism directly affect global network behavior. In this study we set out to determine the consequences of energetic substrate depletion on a network model of human cortical neurons.

Our approach was to develop a combined experimental-computational model sufficiently detailed to be relevant to the problem at hand yet sufficiently simple to provide an intuitive picture of how metabolism governs important aspects of cortical network behavior. For these experiments we used induced cortical glutamatergic neurons (iNs) derived from human embryonic stem cells (hESCs) by overexpression of neurogenin 2 (NGN2) (39) from a genetically safe harbor in order to maximize induction efficiency and improve network

homogeneity (40). We cultured human iNs together with rat astrocytes on multi-electrode arrays (MEAs); extensive characterization of their electrophysiology has been performed previously (39, 41) and suggests individual iNs constitute excitatory cortical layer 2/3 neurons equipped with AMPA receptors. For computational studies we extended a simplified version of the spiking neural network model used by Guerrier *et al.* (2015) to describe the emergence of synchronous bursting driven by synaptic dynamics (42). We found a reduced version of this model captured the same effects and incorporated metabolic regulation of synaptic vesicle recovery in order to interpret experimental data derived from cultured excitatory networks.

Results

Emergence of synchronized bursts during excitatory network development

We cultured human iNs together with rat astrocytes on MEAs from day 3 of induction onwards, from day 12 recording 10mins of electrical activity at three regularly-spaced intervals each week for a total of six weeks (Methods and Materials). To ensure genericity of observed network behavior we repeated this experiment on three separate occasions, each time using a different hESC clone for induction and a new preparation of astrocytes for co-culture. The emergence of spontaneous bursting after 3-4 weeks from induction was a consistent feature of developing networks (Fig. 1). Bursts were easily identified upon visual inspection of recorded data and consisted of a characteristic, high-frequency spike train (Fig. 1A). Timings of bursts were synchronized across all participating electrodes whilst spontaneous action potentials occurring within and between bursts were not. A custom-built synchronous burst detection algorithm (SI Appendix) was used to analyze bursts from raw electrode data and showed that synchronous bursting spread and then stabilized across the network over the course of development. Network maturation was accompanied by a gradual increase in synchronous burst frequency (Fig. 1B), but precise frequencies varied significantly between cultures. Although we do not present an extensive analysis here, we also experienced that, during later stages of network maturation, synchronous bursts underwent different degrees of higher level organization, including the appearance of compound bursting (43) and burst compactification (44).

Several groups have similarly described the emergence of network-wide synchronous bursts in cultures of disassociated primary rat neurons (45-47) and human iNs (48). Based on frequency

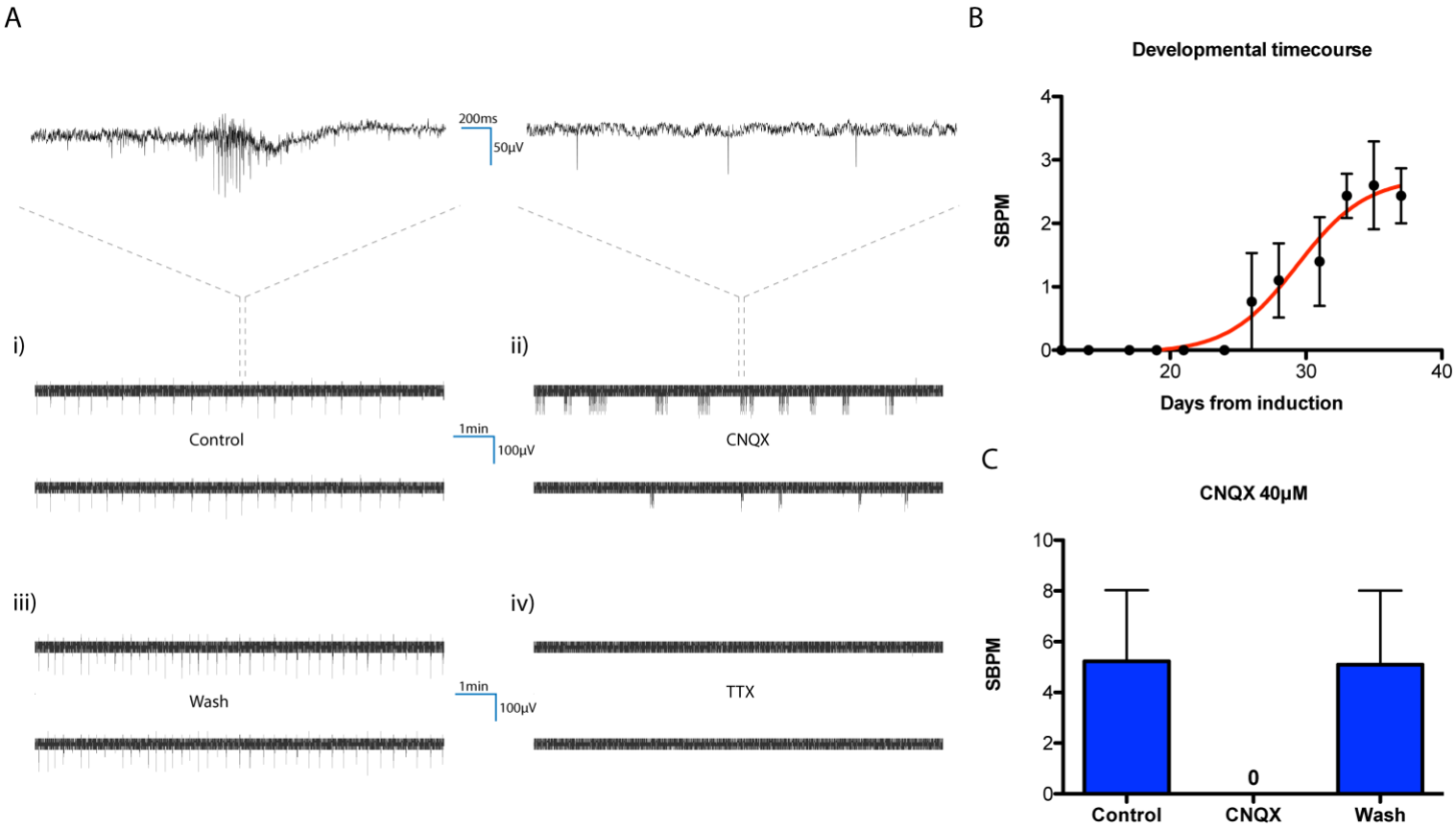

Figure 1. Synchronous bursting characteristics. A) Synchronized bursts consisting of trains of action potentials are clearly visible in raw electrode data. Representative data from two neighboring electrodes showing temporal correlation of bursts occurring in control conditions (i). Synchronized bursts are obliterated (although spontaneous action potentials persist) by the presence of the AMPA/kainite receptor antagonist CNQX (ii), but this effect is immediately reversible following a wash-off (iii). Total inhibition of electrical activity upon treatment with TTX (iv). For illustrative purposes, upper panels displaying fast time scale are smoothed using a 2ms Gaussian window. **B)** Number of synchronous bursts per minute (SBPM) gradually increases and stabilizes over the course of network development (data from three independent 6-week-long experiments each using distinct hESC clones and astrocyte preparations). TWANOVA reports a p-value $P_{condition} < 0.0001$ for time (days from induction) as the major source of variation. **C)** Same cultures subjected to CNQX treatment once mature reveals dependence of synchronous bursting on excitatory glutamatergic signaling. Zero synchronous bursts were observed in the presence of CNQX.

range alone, the description of bursting provided by Frega et al. (48) appears closely related. This is perhaps expected given that iNs were used in those experiments also, but one cannot rule out possible differences caused by viral targeting or contributions from excitatory/inhibitory neuronal contamination in astrocyte preparations (49). To confirm that synchronous bursts are dependent on excitatory glutamatergic signaling we subjected each culture to treatment with 40μM cyanquixaline (CNQX) following the developmental time course. CNQX is a specific, competitive inhibitor of excitatory AMPA/kainite receptors (50). 10mins incubation of cultures in the presence of this drug resulted in total inhibition of synchronous bursts without affecting spontaneous firing of action potentials (Fig. 1A, 1C and S1) (see also Supplementary Dataset 1). The effect was immediately reversible following a single wash with fresh media. Subsequent administration of 1μM tetrodotoxin (TTX), a potent voltage-gated sodium channel blocker, silenced the network entirely (Fig. 1A and S1) (see also Supplementary Dataset 1). Conversely, administration of 40μM bicuculline, a competitive antagonist of the primary inhibitory GABA receptor, had no detectible effect on synchronous bursts (not shown).

Kinetics of vesicle recycling regulate synchronous bursting frequency

Having confirmed that neural communication *via* release of the excitatory neurotransmitter glutamate is responsible for coordinating synchronous bursting, we were interested to know what aspects of neurotransmission regulate synchronous burst frequency. To evaluate the role of the synaptic vesicle cycle we sought to inhibit mechanisms known to be important for vesicle recovery and replenishment following exocytosis. Various pathways and vesicle pools are suggested to participate in synaptic vesicle recycling (33, 34), and the currently accepted knowledge is concisely summarized by KEGG pathway entry hsa04721. Common to all pathways is vesicle re-acidification by the Vacuolar-type ATPase (V-ATPase) required to generate the electrochemical proton gradient that is an essential prerequisite for the uptake of glutamate into synaptic vesicles (51, 52). Dynamin is primarily responsible for vesicle scission during endocytosis, but its role might not be universal (53), particularly in faster recycling pathways such as kiss-and-run (34, 54).

We evaluated the response of cultures to acute pharmacological inhibition of proteins implicated with a role in synaptic vesicle recycling by repeated rounds of 10min incubation in media treated with drug or vehicle, transfer to the MEA recording device for a 200sec

equilibration, and a 10min recording of network activity (Methods and Materials). We found that 50nM concanamycin A (CMA), a highly specific inhibitor of the V-ATPase (55), significantly reduced the number of synchronous bursts per minute (SBPM) (Fig. 2A, vehicle: 6.57 ± 0.78; CMA: 0.30 ± 0.15) suggesting the rate of vesicular re-acidification is a key determinant of synchronous bursting frequency. Conversely, treatment with 80µM dynasore (56), an inhibitor of all the major dynamin isoforms, had no significant effect after the first or second 10min incubation (Fig. 2B, vehicle: 3.80 ± 1.00; dynasore 10min: 4.43 ± 1.11; dynasore 20min: 3.97 ± 1.47). From this we concluded that the rate of synaptic vesicle recycling regulates the frequency of network-wide synchronous activity, and that the efficiency of re-acidification required for vesicular neurotransmitter uptake plays a key role in this regulatory process. Although we cannot completely exclude the involvement of dynamin-mediated endocytosis in synchronous bursting, a parsimonious interpretation of our observations is that the increased level of synaptic vesicle turnover required to support synchronous bursting occurs *via* a fast, dynamin-independent pathway.

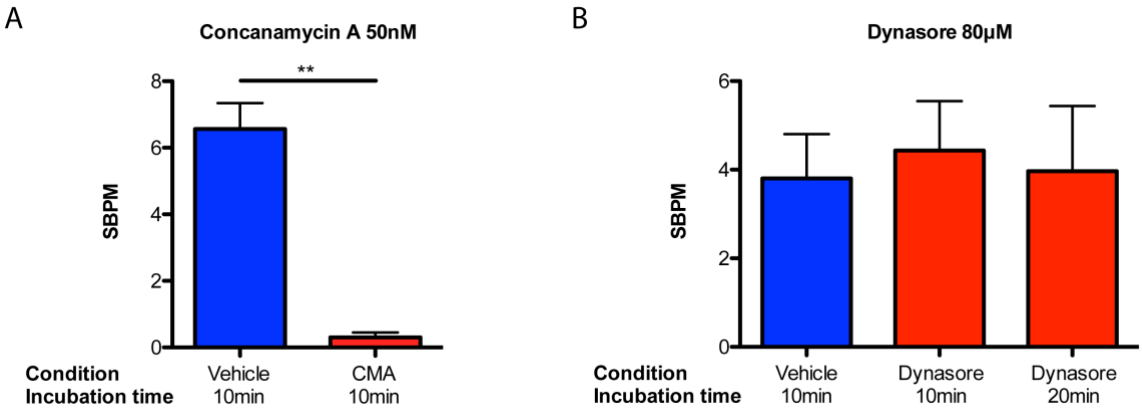

Figure 2. Inhibiting vesicle recovery pathways. A) Incubating cultures in the presence of 50nM CMA for 10min significantly reduces the frequency of synchronous bursting compared to 10min incubation in the presence of vehicle alone. CMA *versus* vehicle P = 0.0014; $P_{condition}$ = 0.0128; N=3. Conversely, **B)** 80µM dynasore had no detectible effect on SBPM after the first, or second, 10min incubation. Dynasore 10min *versus* vehicle P = 0.69, dynasore 20min *versus* vehicle P = 0.93; $P_{condition}$ = 0.38; N=3.

Glucose depletion reduces synchronous burst rate

To assess the consequences of energetic substrate restriction on synchronous bursting we developed a timing-based protocol of substrate depletion and repletion (Fig. 3A and Methods and Materials). On the basis of recent work, 20-30min in the absence of extracellular glucose

is sufficient to impair presynaptic transmission (37, 38, 57), which is far shorter than the 16h time window in which the survival of cultured neurons remains uncompromised (58). As with previous pharmacological experiments, we repeated multiple rounds of 10min incubation, 200sec equilibration, followed by a 10min recording after which transfer of a culture into fresh media was always performed regardless as to whether or not it contained an alternative mix of substrates (Fig. 3A and Methods and Materials). This was to rule out any confounding effects of mechanical perturbation or media acidification/oxygenation. We found that synchronous burst frequency (as measured by SBPM) decreased following the first 10min incubation in the absence of 25mM glucose and 0.22mM pyruvate and was significantly reduced after the second 10min incubation, with far fewer synchronous bursts occurring at regularly-spaced intervals across the subsequent 10min recording (Fig. 3B and S2, glucose and pyruvate: 6.30 ± 1.85; no substrate 10min: 4.85 ± 1.10; no substrate 20min: 0.425 ± 0.24) (see also Supplementary Dataset 2). This phenomenon was significantly reversed after the reintroduction of 25mM glucose alone (Fig. 3B and S2, glucose alone: 4.05 ± 1.10) (see also Supplementary Dataset 2), indicating that a high SBPM can be sustained in absence of the oxidative substrate pyruvate.

In order to confirm our observations are not related to the artificially high levels of glucose (25mM) conventionally used in cell culture media, a consequence of osmotic stress, or complete absence of an alternative oxidative substrate, we repeated the substrate depletion-repletion protocol under physiologically-relevant conditions (59). We retained 0.22mM pyruvate and supplemented with 5mM DL-lactate (racemic mixture) at all time points, reducing the total concentration of extracellular glucose to 5mM. To control for the possible effect of osmotic stress during periods of glucose depletion we replaced D-glucose with its non-metabolically-active isoform L-glucose. In accordance with previous experiments, we found that substituting 5mM D-glucose with 5mM L-glucose led to a slight decrease in synchronous burst frequency after 10min incubation followed by a significant drop in SBPM during the second 10min recording (Fig. 3C and S3, D-glucose: 5.70 ± 0.30; L-glucose 10min: 2.60 ± 0.10; L-glucose 20min: 0.6 ± 0.20) (see also Supplementary Dataset 3). This effect was significantly reversed upon re-substitution of L-glucose with D-glucose (Fig. 3C and S3, D-glucose replenishment: 4.05 ± 0.25) (see also Supplementary Dataset 3), confirming that the metabolically active form of glucose alone can sustain a high synchronous bursting frequency. The continued presence of substrates that can only be used to generate ATP by oxidative phosphorylation implies ATP generated by glycolysis is required to sustain a high SBPM. This

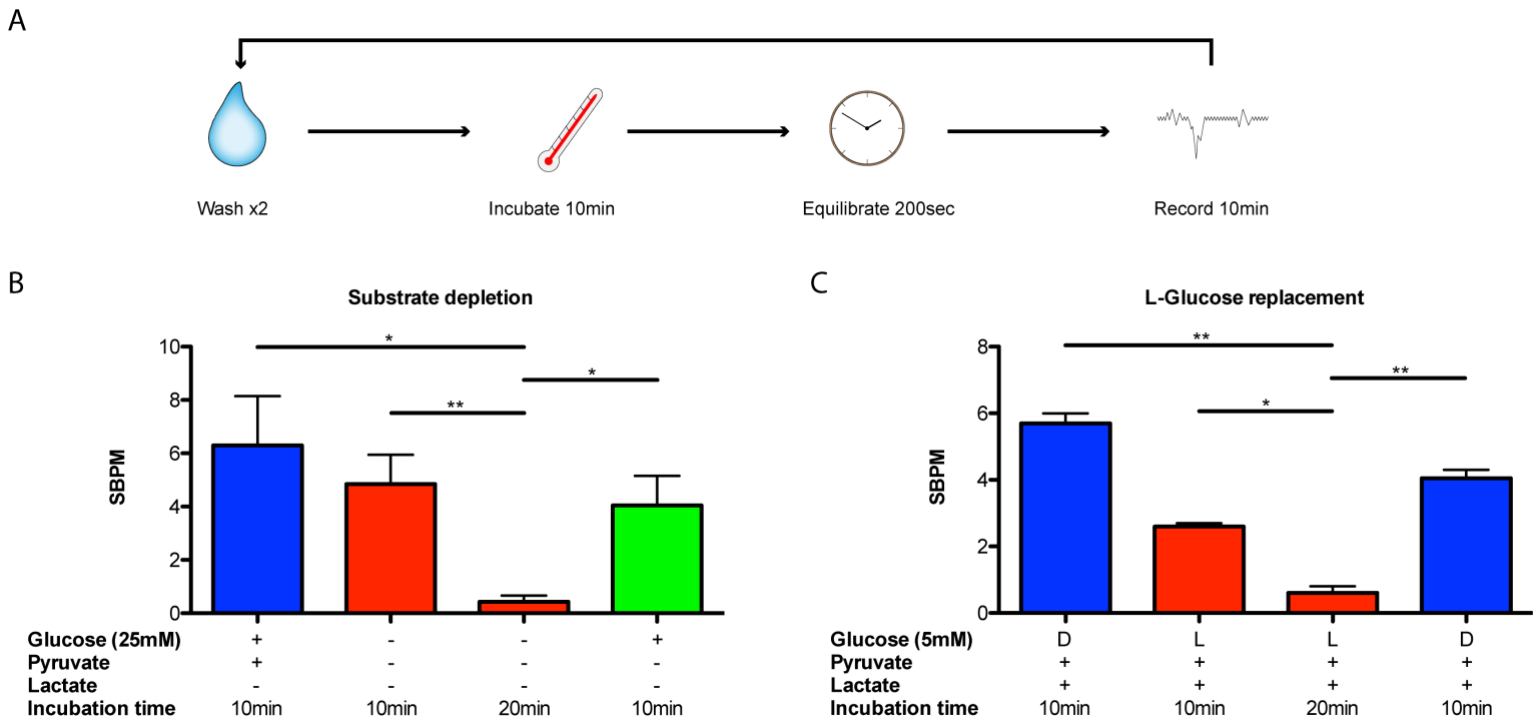

Figure 3. Glucose depletion decreases SBPM. A) Cartoon schematic of substrate depletion-repletion experimental protocol described in Methods and Materials. Each wash-incubate-equilibrate-record epoch was performed using fresh media regardless of substrate composition. **B)** Synchronous burst frequency decreases following 10min incubation in the absence of extracellular glucose (25mM) and pyruvate (0.22mM), and significantly further still following a second 10min incubation. Replenishment of glucose alone is sufficient to restore a significantly higher SBPM. No substrate 20min *versus* glucose and pyruvate P = 0.0196; no substrate 20min *versus* no substrate 10min P = 0.0076; glucose alone *versus* no substrate 20min P = 0.0183; $P_{condition}$ = 0.0015; N=4. **C)** Only the metabolically active D-isoform of glucose (not L-glucose) can sustain a significantly higher SBPM in physiologically-relevant conditions containing 5mM D- or L-glucose, 5mM DL-lactate (racemic mixture) and 0.22mM pyruvate. L-glucose 20min *versus* D-glucose control P = 0.0050; L-glucose 20min *versus* L-glucose 10min P = 0.0123; D-glucose replenishment *versus* L-glucose 20min P = 0.0085; $P_{condition}$ = 0.0027; N=2.

was further supported by substituting 5mM glucose for 5mM galactose, a substrate whose transport and pre-processing means it passes through glycolysis more slowly (Chapter 16.1.11. in (60)), which also failed to rescue the higher synchronous bursting frequency (Fig. S4) (see also Supplementary Dataset 4).

Computational model of an excitatory network with metabolically-regulated STSP

Our experimental results using CNQX to inhibit synaptic transmission suggest that network-wide synchronous bursts are an emergent property of excitatory synaptic communication rather than synchronization of intrinsically bursting neurons. A key component of the mechanism regulating synchronous burst frequency is the timescale of synaptic vesicle recovery following synaptic depression (SD), and so we implemented a model that captures all these features (42). Guerrier *et al*. (2015) describe a network of excitatory neurons based on random, sparse synaptic connections equipped with SD and synaptic facilitation (SF). The incorporation of short-time synaptic plasticity (STSP) is a refinement of the classical STSP model (61), based on the existence of three vesicle pools, which can generate endogenous synchronous bursting initiated by spontaneous action potential firing. However, in light of considerable ambiguity surrounding the precise nature of vesicle pools and recycling pathways involved, we explored the possibility of simplifying STSP dynamics further and found that a single pool of vesicles (Fig. 4A) is sufficient to recapitulate the synchronous bursting phenotype we observed experimentally (SI Appendix).

Following the approach of Lucas *et al*. (38), we extended our computational model to include metabolic regulation of the rate of synaptic vesicle recovery. The principle that replenishment of vesicle pools occurs on a slower timescale in low glucose conditions is based on the observed effect that substrate depletion has on individual presynapses (20, 37, 38). We modified the time constant of vesicle recovery to account for the fact that under low glucose conditions, when energy charge (ATP:ADP/AMP ratio) is more sensitive to increased ATP consumption rates, efficacies of synaptic vesicle endocytosis and re-acidification become compromised (26-28, 31, 32). We found that, when the rate of vesicle recovery is lowered in response to a decrease in extracellular glucose concentration, there is a corresponding decrease in synchronous burst frequency (Fig. 4B) as we observed experimentally. Our computational model therefore provides a framework for understanding how the capacity for local presynaptic ATP production determines the efficiency with which information can be propagated throughout a neuronal network.

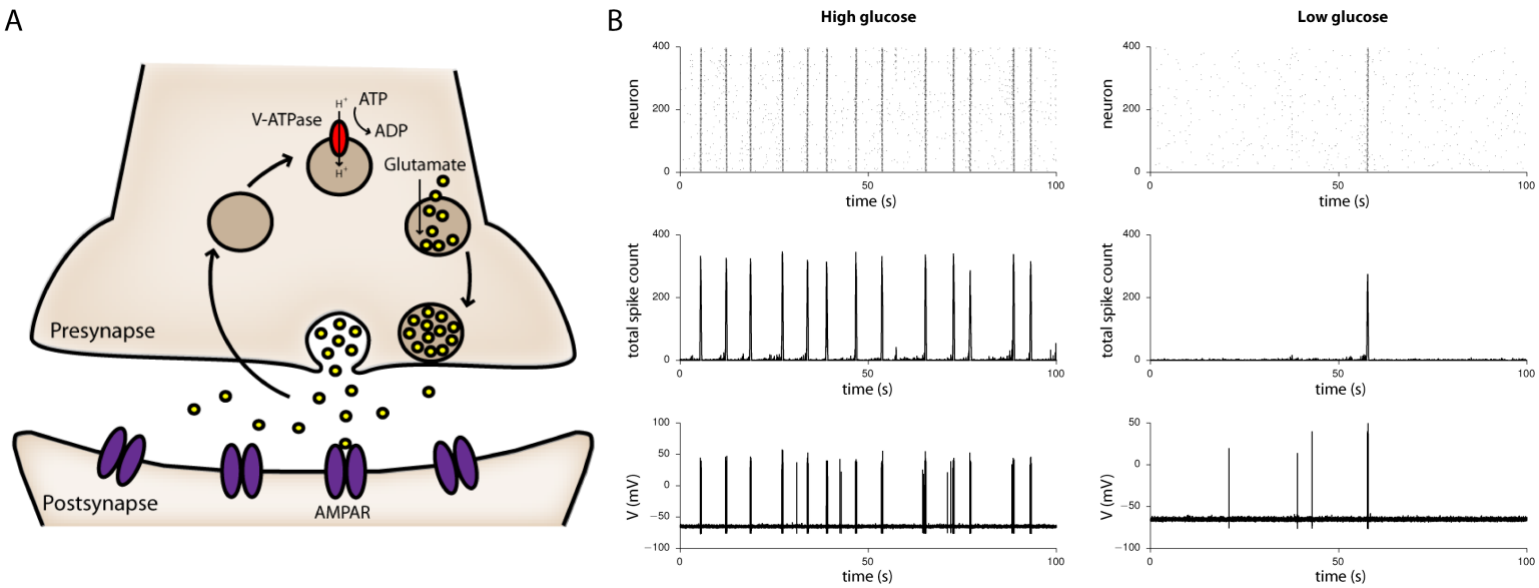

Figure 4. Computational model of synchronous bursting. A) Cartoon schematic showing that presynaptic vesicle recycling involves several steps suggested to depend on ATP supplied by glycolysis, including endocytosis and vesicle re-acidification by the V-ATPase. In our computational model we encompassed contributions from all pathways in a single term describing the rate of synaptic vesicle recovery. The rate of synaptic vesicle recovery is significantly reduced in the absence of extracellular glucose. **B)** Simulations reveal that in high levels of extracellular glucose (left), synchronized bursting persists at a relatively high frequency compared to that in low levels of extracellular glucose (right). Upper panels display raster plots of spike timings from all 400 neurons in the simulated network, middle panels the total spike count across the network as a function of time, and lower panels the corresponding fluctuations in the membrane potential of a representative neuron.

Discussion

We have used cultured networks of excitatory human iNs and rat astrocytes combined with computational modelling to reveal how energetic substrate availability influences global network behavior. Glucose depletion dramatically reduced the prevalence of network-wide synchronous bursts mediated by excitatory neurotransmission, an effect that could not be rescued by a purely respiratory substrate such as lactate or pyruvate. Our results build upon earlier work focused on the effects of glycolytic metabolites on neuronal function, which revealed that glucose is essential for synaptic transmission even though intracellular ATP levels remain normal in the presence of oxidative fuel sources (62-65). This dependence on glucose could be particularly relevant at the presynapse, where the majority of nerve terminals lack mitochondria (24, 25) suggesting that presynaptic ATP supply is predominantly glycolytic.

Our results also reveal that the rate of synaptic vesicle recovery is a key determinant of synchronous bursting frequency. In light of recent evidence that fully-functional presynaptic transmission is dependent on activity-induced glycolysis (26-28, 31, 32), these data support the proposal that a rapid supply of ATP is required to power the synaptic vesicle cycle necessary to maintain a high SBPM. This is further supported by studies that demonstrate a decrease in vesicle recovery rates at individual synapses in the absence of glucose (37, 38), but we note other factors such as the inability of the presynaptic action potential to trigger vesicle release cannot be fully excluded (57). Our experiments also do not completely rule out the possibility that postsynaptic function is impaired in cultures lacking glucose, since reduced excitatory postsynaptic action potential propagation would also lead to a decrease in SBPM. However, the short length of time spent in the absence of extracellular glucose, the ability of networks to continue firing spontaneous action potentials throughout this period, and the immediate recovery following glucose replenishment, suggest that postsynaptic responses remain largely unaffected. Postsynaptic neurons have considerable energy requirements associated with reversal of ion fluxes and membrane potential maintenance, but ATP for these processes is thought to be supplied almost exclusively *via* oxidative metabolism (3-5).

Based on pharmacological inhibition of the V-ATPase, a plausible explanation for the observed decrease in SBPM when glucose is depleted would be the slower rate of re-acidification required for glutamate uptake into synaptic vesicles. Strikingly, this step of the synaptic vesicle cycle has been suggested to be predominantly dependent on glycolysis (31, 32), which can

supply ATP at a rate far higher than oxidative phosphorylation (35, 36). Our data are therefore consistent with the hypothesis that V-ATPase activity diminishes when glycolytic flux is reduced, which would in turn explain the decrease in synchronous burst frequency. However, other stages of vesicle recycling, such as endocytosis, are likewise energetically demanding processes that depend on oxidative (66) or non-oxidative supply of ATP (26, 28). In our computational model we attempted to remain agnostic- given the lack of conclusive experimental evidence for the involvement of different pathways during synaptic vesicle recycling (33, 34). We found that a reduction in the overall rate of vesicle recovery is sufficient to explain the decrease of synchronous network activity in response to glucose depletion, but further work will be required to elucidate the various contributions from each pathway. Although we found that dynasore treatment had no significant effect on SBPM, one cannot rule out possible contributions from endocytosis, potentially involving a dynamin-independent mechanism (53).

In summary, our results reveal how synchronous network activity is affected by energy substrate restriction, which is to our knowledge the first explicit demonstration of a global network response to underlying changes in synaptic metabolism. Our study therefore attempts a first step towards bridging the gap in understanding between metabolic regulation at the synapse and spatiotemporal coupling of hemodynamics to synchronous neural activity within the cortex (67). By making experimental data and computational code available to the wider community, we hope to advance theoretical knowledge on the role of metabolism and synchronization in energy-efficient neural coding (e.g. (68-70)). Finally, our combined experimental-computational approach paves the way for establishing an effective and pragmatic model for (dys)regulation of metabolism in the (un)healthy human brain.

Methods and Materials

Cell culture

Human embryonic stem cells H9 [Wisconsin International Stem Cell (WISC) Bank, WiCell Research Institute, WA09 cells] were cultured according to WiCell stem cell protocols in 6-well plates on Matrigel (Corning, hESC-Qualified) in StemFlex (Gibco). Use of stem cell line H9 was approved by the Steering Committee of the UK Stem Cell Bank and for the Use of Stem Cell Lines (ref: SCSC18-05).

Primary mixed glial cultures were derived from P0-P2 neonatal Spraque Dawley rats and were generated along the previous guidelines (71), with minor modifications (72). The pups were euthanized following Schedule 1 rules and regulations from the Home Office Animal Procedures Committee UK (APC). Mixed glia cells were maintained for 10 days in culture after which flasks were shaken for 1h at 260rpm on an orbital shaker to remove the loosely attached microglia, and then overnight at 260rpm to dislodge oligodendrocyte precursors. Astrocyte cultures were then maintained in glial culture medium (Dulbecco's Modified Eagle's Medium (DMEM) supplemented with 10% FBS (Fetal Bovine Serum), glutamine and 1% Pen/Strep) and passaged at a ratio of 1:3, every 10-14 days. Cells were passaged at least once before co-culturing with iNs and were only used between passages 2 and 5.

Induction of NGN2- hESCs and culturing iNs on MEAs

Gene targeting and generation of dual GSH-targeted NGN2 OPTi-OX hESCs was performed as described previously (40). The day prior to initiation of the reprogramming process (day 0), NGN2-hESC colonies grown to 70-80% confluency were disassociated using Accutase (Sigma-Aldrich) and isolated NGN2- hESCs were seeded in 6-well plates at a density of 25,000cells/cm^2 on Matrigel (Corning, hESC-Qualified) in StemFlex (Gibco) supplemented with RevitaCell (Gibco). Inducible overexpression of NGN2 began on day 1 by transferring cells into D0-2 induction medium (DMEM/F12, 1% Pen/Strep, 1x non-essential amino acid solution (NEAA, Gibco), 1% (v/v) N-2 supplement (Gibco), 1x Glutamax (Gibco), and doxycycline (dox) at 4μg/ml). On day 3, cells were dissociated using Accutase and re-suspended at a density of 4000cells/μl in >D2 medium (Neurobasal-A Medium (ThermoFisher), 1% Pen/Strep, 1x Glutamax, 1x B27 Supplement (Gibco), 10ng/ml brain-derived neurotrophic factor (BDNF), 10ng/ml human recombinant neurotrophin-3 (NT-3), and dox at 4μg/ml) supplemented with RevitaCell. Rat astrocytes were dissociated using 0.05% trypsin-ethylenediaminetetraacetic acid (EDTA) and re-suspended at a density of 4000cells/μl in >D2 medium supplemented with RevitaCell. Astrocytes were then mixed at a ratio of 1:1 with dox-treated NGN2- hESCs in >D2 to make a final seeding density of 2000cells/μl for each cell type.

Cells were seeded onto a selection of 8x8(60 electrodes in total, excluding corners)-electrode MEAs (60MEA200/30iR-Ti or 60ThinMEA100/10iR-ITO, Multichannel Systems) covered by Teflon-sealed lids (Multichannel Systems) and pre-coated overnight at 4°C with 500μg/ml

poly-D-lysine (PDL) in ultrapure water. For seeding, MEAs were first incubated for 1h at 37°C, 5% CO_2 with a 20µl drop of laminin solution (20µg/ml laminin in DMEM) covering the electrode region. The laminin drop was aspirated immediately prior to seeding and replaced with a 15µl drop of re-suspended cell mixture (total density of 4000cells/µl). MEAs were incubated with 15µl drops of cell suspension for 1h at 37°C, 5% CO_2 to allow cells to adhere before being topped up to 1ml with >D2 medium (without RevitaCell). Cultures were maintained throughout lifespan at 37°C, 5% CO_2 with 500µl media replenished every second day. 2µM cytosine β-D-arabinofuranoside was added to cultures on day 5 to inhibit astrocyte proliferation and kill undifferentiated NGN2- hESCs, and dox was excluded from >D2 media from day 8 onward.

Recording procedures

For recordings, MEAs incubated at 37°C, 5% CO_2 were transferred to the MEA recording device (MEA2100-2x60-System, Multichannel Systems). All recordings were performed in atmospheric conditions with stage and custom-built heated lid held at 37°C. Developmental time course recordings took place every second or third day, 10mins after a 37°C, 5% CO_2 incubation following half-media change. MEAs were allowed to equilibrate for 200sec on the MEA recording device and recording sessions lasted 10mins with local field potentials from all electrodes sampled at 25kHz.

A strict regime of media exchange, incubation, equilibration, and recording was enforced for all pharmacological and substrate depletion-repletion experiments. For drug treatments, MEA cultures were first washed (2x total media exchange) in >D2 media with vehicle (all drugs were diluted in DMSO or ddH_2O as required for treatment and corresponding concentration of the dissolving agent used as vehicle controls) to control for the effects of mechanical perturbation, and subsequently incubated at 37°C, 5% CO_2 for precisely 10min. MEAs were then transferred to the recording device (pre-heated to 37°C) and equilibrated for 200sec prior to a 10min recording sampling at 25kHz. This procedure was repeated, immediately following each recording, under the multiple test conditions (inclusion of pharmacological compound in fresh >D2 media) necessary for each experiment. Cultures were exchanged into fresh >D2 media on termination of the final recording and returned to incubation at 37°C, 5% CO_2. The same protocol was employed for substrate depletion-repletion experiments using >D2 media based on Neurobasal-A medium lacking glucose and sodium pyruvate (ThermoFisher). In this case

media supplemented with the appropriate combinations of 25 or 5mM D- or L-glucose, 0.22mM sodium pyruvate, 5mM sodium DL-lactate (racemic mixture), and 5mM D-galactose served as test conditions.

Recorded data were processed and analyzed using the MC Rack/MC Tools software (Multichannel Systems) and a custom-built synchronous burst detection algorithm described in the SI Appendix. The algorithm calculates the number of synchronous bursts per minute (SBPM) for each recording and was used to extract this value from all biological replicates and conditions for further statistical analysis. Two-way analysis of variance (TWANOVA) was performed in GraphPad Prism to assess the influence of biological conditions (time, energy substrate composition, or drug) and biological replicates (N = number of cultures) on SBPM; resulting p-values for conditions ($P_{condition}$) and number of replicates for each experiment are displayed in the figure legends. Student's t-tests were used to compare mean SBPMs from pairs of biological conditions relevant to experimental interpretation; corresponding p-values are displayed in figure legends and annotated in figures with * signifying $P < 0.05$ and ** signifying $P < 0.01$. Error bars are standard error of the mean (SEM) and SBPM values reported in main text are mean ± SEM. Representational experimental data (Supplementary Datasets 1-4) have been deposited in Figshare (see Data Deposition for link and DOIs).

Computational modelling

We simulated a modified version of the excitatory neural network model described by Guerrier *et al*. (42) consisting of 20x20 (400) connected neurons organized on a square lattice. Membrane potential of each neuron was modelled using the simplified Hodgkin-Huxley model and neurons were connected randomly according to a probability distribution that decays as a function of distance between pairs on neurons (see SI Appendix and (42)). We believe this type of random synaptic connectivity accurately reflects that which emerges in our experimental cultures over the course of development. In the original work (42), the fraction of available *free*, *docked*, and *recovering* synaptic vesicles are simulated, corresponding to the proposed existence of multiple vesicle pools and recovery pathways (33, 34). Here we simulated only the fraction of docked vesicles, assuming that recovery is described by a single rate constant encompassing these mechanisms, and have shown that this is sufficient to recapitulate the emergence of synchronous bursting across the simulated network (SI Appendix). To model the effect of glucose depletion on synaptic vesicle recovery, we allow for modulation of this rate

by energy substrate availability, assuming that when the levels of extracellular glucose are low the overall rate of recovery decreases as a function of recent presynaptic energy consumption. Although we take inspiration from a similar approach used in (38), we do not intend to model the exact functional form of this glucose dependence and instead sought only to capture the desired properties using a simplified model of presynaptic metabolism (SI Appendix).

Supplementary Information

Supplementary Information accompanying this manuscript includes:
SI Appendix
Figures S1- S4
Table S1

Acknowledgements

We thank past and present members of the O'Neill and Kotter labs for assistance and comments. We are grateful to Simon Laughlin for inspiring discussions and suggestions. DST is a Simons Foundation Fellow of the Life Sciences Research Foundation. MKAK is supported by a Daya Diri-Cambridge Trust Scholarship. Research in MRNK's laboratory is funded by the UK Multiple Sclerosis Society and supported by a core support grant from the Wellcome Trust and Medical Research Council to the Wellcome Trust-MRC Cambridge Stem Cell Institute. MRNK holds a National Institute for Health Research Clinician Scientist Award CS-2015-15-023 (Disclaimer: This report is independent research arising from Clinician Scientist Award, CS-2015-15-023, supported by the National Institute for Health Research. The views expressed in this publication are those of the authors and not necessarily those of the National Health Service, National Institute for Health Research or the Department of Health). JSO is supported by the Medical Research Council (MC_UP_120/4).

Author Contributions

DST conceived study and designed experiments with support from MRNK and JSO. DST and MKAK performed cell culture and developmental time course experiments; DST performed substrate replacement and drug treatment experiments; DST analyzed the data. RE and DST developed computational model; RE performed simulations. DST wrote the paper with input from all authors.

Data Deposition

Representational multi-electrode array data have been deposited in Figshare (https://figshare.com) and are publicly available at the following DOIs: 10.6084/m9.figshare.6741464 (Supplementary Dataset 1); 10.6084/m9.figshare.6741479 (Supplementary Dataset 2); 10.6084/m9.figshare.6741485 (Supplementary Dataset

3); 10.6084/m9.figshare.6741494 (Supplementary Dataset 4). Computational code available in GitHub: https://github.com/r-echeveste/meta_reg_net.

References

1. Ames A, 3rd (2000) CNS energy metabolism as related to function. *Brain Res Brain Res Rev* 34(1-2):42-68.
2. Mink JW, Blumenschine RJ, & Adams DB (1981) Ratio of central nervous system to body metabolism in vertebrates: its constancy and functional basis. *Am J Physiol* 241(3):R203-212.
3. Attwell D & Laughlin SB (2001) An energy budget for signaling in the grey matter of the brain. *J Cereb Blood Flow Metab* 21(10):1133-1145.
4. Lennie P (2003) The cost of cortical computation. *Curr Biol* 13(6):493-497.
5. Harris JJ, Jolivet R, & Attwell D (2012) Synaptic energy use and supply. *Neuron* 75(5):762-777.
6. Levy WB & Baxter RA (1996) Energy efficient neural codes. *Neural Comput* 8(3):531-543.
7. Perge JA, Koch K, Miller R, Sterling P, & Balasubramanian V (2009) How the optic nerve allocates space, energy capacity, and information. *J Neurosci* 29(24):7917-7928.
8. Levy WB & Baxter RA (2002) Energy-efficient neuronal computation via quantal synaptic failures. *J Neurosci* 22(11):4746-4755.
9. Laughlin SB & Sejnowski TJ (2003) Communication in neuronal networks. *Science* 301(5641):1870-1874.
10. Attwell D, *et al.* (2010) Glial and neuronal control of brain blood flow. *Nature* 468(7321):232-243.
11. Nortley R & Attwell D (2017) Control of brain energy supply by astrocytes. *Curr Opin Neurobiol* 47:80-85.
12. Chih CP, Lipton P, & Roberts EL, Jr. (2001) Do active cerebral neurons really use lactate rather than glucose? *Trends Neurosci* 24(10):573-578.
13. Chih CP & Roberts EL, Jr. (2003) Energy substrates for neurons during neural activity: a critical review of the astrocyte-neuron lactate shuttle hypothesis. *J Cereb Blood Flow Metab* 23(11):1263-1281.

14. Barros LF & Weber B (2018) CrossTalk proposal: an important astrocyte-to-neuron lactate shuttle couples neuronal activity to glucose utilisation in the brain. *J Physiol* 596(3):347-350.
15. Fox PT, Raichle ME, Mintun MA, & Dence C (1988) Nonoxidative glucose consumption during focal physiologic neural activity. *Science* 241(4864):462-464.
16. Pellerin L & Magistretti PJ (1994) Glutamate uptake into astrocytes stimulates aerobic glycolysis: a mechanism coupling neuronal activity to glucose utilization. *Proc Natl Acad Sci U S A* 91(22):10625-10629.
17. Magistretti PJ & Allaman I (2018) Lactate in the brain: from metabolic end-product to signalling molecule. *Nat Rev Neurosci* 19(4):235-249.
18. Schurr A, West CA, & Rigor BM (1988) Lactate-supported synaptic function in the rat hippocampal slice preparation. *Science* 240(4857):1326-1328.
19. Izumi Y, Benz AM, Katsuki H, & Zorumski CF (1997) Endogenous monocarboxylates sustain hippocampal synaptic function and morphological integrity during energy deprivation. *J Neurosci* 17(24):9448-9457.
20. Bak LK, Schousboe A, Sonnewald U, & Waagepetersen HS (2006) Glucose is necessary to maintain neurotransmitter homeostasis during synaptic activity in cultured glutamatergic neurons. *J Cereb Blood Flow Metab* 26(10):1285-1297.
21. Patel AB, *et al.* (2014) Direct evidence for activity-dependent glucose phosphorylation in neurons with implications for the astrocyte-to-neuron lactate shuttle. *Proc Natl Acad Sci U S A* 111(14):5385-5390.
22. Lundgaard I, *et al.* (2015) Direct neuronal glucose uptake heralds activity-dependent increases in cerebral metabolism. *Nat Commun* 6:6807.
23. Diaz-Garcia CM, *et al.* (2017) Neuronal Stimulation Triggers Neuronal Glycolysis and Not Lactate Uptake. *Cell Metab* 26(2):361-374 e364.
24. Shepherd GM & Harris KM (1998) Three-dimensional structure and composition of CA3-->CA1 axons in rat hippocampal slices: implications for presynaptic connectivity and compartmentalization. *J Neurosci* 18(20):8300-8310.
25. Chavan V, *et al.* (2015) Central presynaptic terminals are enriched in ATP but the majority lack mitochondria. *PLoS One* 10(4):e0125185.
26. Rangaraju V, Calloway N, & Ryan TA (2014) Activity-driven local ATP synthesis is required for synaptic function. *Cell* 156(4):825-835.
27. Ashrafi G, Wu Z, Farrell RJ, & Ryan TA (2017) GLUT4 Mobilization Supports Energetic Demands of Active Synapses. *Neuron* 93(3):606-615 e603.

28. Jang S, *et al.* (2016) Glycolytic Enzymes Localize to Synapses under Energy Stress to Support Synaptic Function. *Neuron* 90(2):278-291.
29. Knull HR (1980) Compartmentation of glycolytic enzymes in nerve endings as determined by glutaraldehyde fixation. *J Biol Chem* 255(13):6439-6444.
30. Takamori S, *et al.* (2006) Molecular anatomy of a trafficking organelle. *Cell* 127(4):831-846.
31. Ikemoto A, Bole DG, & Ueda T (2003) Glycolysis and glutamate accumulation into synaptic vesicles. Role of glyceraldehyde phosphate dehydrogenase and 3-phosphoglycerate kinase. *J Biol Chem* 278(8):5929-5940.
32. Ishida A, Noda Y, & Ueda T (2009) Synaptic vesicle-bound pyruvate kinase can support vesicular glutamate uptake. *Neurochem Res* 34(5):807-818.
33. Sudhof TC (2004) The synaptic vesicle cycle. *Annu Rev Neurosci* 27:509-547.
34. Alabi AA & Tsien RW (2013) Perspectives on kiss-and-run: role in exocytosis, endocytosis, and neurotransmission. *Annu Rev Physiol* 75:393-422.
35. Pfeiffer T, Schuster S, & Bonhoeffer S (2001) Cooperation and competition in the evolution of ATP-producing pathways. *Science* 292(5516):504-507.
36. Ashrafi G & Ryan TA (2017) Glucose metabolism in nerve terminals. *Curr Opin Neurobiol* 45:156-161.
37. Sobieski C, Fitzpatrick MJ, & Mennerick SJ (2017) Differential Presynaptic ATP Supply for Basal and High-Demand Transmission. *J Neurosci* 37(7):1888-1899.
38. Lucas SJ, *et al.* (2018) Glucose and lactate as metabolic constraints on presynaptic transmission at an excitatory synapse. *J Physiol* 596(9):1699-1721.
39. Zhang Y, *et al.* (2013) Rapid single-step induction of functional neurons from human pluripotent stem cells. *Neuron* 78(5):785-798.
40. Pawlowski M, *et al.* (2017) Inducible and Deterministic Forward Programming of Human Pluripotent Stem Cells into Neurons, Skeletal Myocytes, and Oligodendrocytes. *Stem Cell Reports* 8(4):803-812.
41. Lam RS, Topfer FM, Wood PG, Busskamp V, & Bamberg E (2017) Functional Maturation of Human Stem Cell-Derived Neurons in Long-Term Cultures. *PLoS One* 12(1):e0169506.
42. Guerrier C, Hayes JA, Fortin G, & Holcman D (2015) Robust network oscillations during mammalian respiratory rhythm generation driven by synaptic dynamics. *Proc Natl Acad Sci U S A* 112(31):9728-9733.

43. Bertram R, Satin L, Zhang M, Smolen P, & Sherman A (2004) Calcium and glycolysis mediate multiple bursting modes in pancreatic islets. *Biophys J* 87(5):3074-3087.

44. Paavilainen T, *et al.* (2018) Effect of prolonged differentiation on functional maturation of human pluripotent stem cell-derived neuronal cultures. *Stem Cell Res* 27:151-161.

45. Wagenaar DA, Pine J, & Potter SM (2006) An extremely rich repertoire of bursting patterns during the development of cortical cultures. *BMC Neurosci* 7:11.

46. Eytan D & Marom S (2006) Dynamics and effective topology underlying synchronization in networks of cortical neurons. *J Neurosci* 26(33):8465-8476.

47. Pasquale V, Massobrio P, Bologna LL, Chiappalone M, & Martinoia S (2008) Self-organization and neuronal avalanches in networks of dissociated cortical neurons. *Neuroscience* 153(4):1354-1369.

48. Frega M, *et al.* (2017) Rapid Neuronal Differentiation of Induced Pluripotent Stem Cells for Measuring Network Activity on Micro-electrode Arrays. *J Vis Exp* (119).

49. Hildebrand B, Olenik C, & Meyer DK (1997) Neurons are generated in confluent astroglial cultures of rat neonatal neocortex. *Neuroscience* 78(4):957-966.

50. Blake JF, Brown MW, & Collingridge GL (1988) CNQX blocks acidic amino acid induced depolarizations and synaptic components mediated by non-NMDA receptors in rat hippocampal slices. *Neurosci Lett* 89(2):182-186.

51. Maycox PR, Deckwerth T, Hell JW, & Jahn R (1988) Glutamate uptake by brain synaptic vesicles. Energy dependence of transport and functional reconstitution in proteoliposomes. *J Biol Chem* 263(30):15423-15428.

52. Naito S & Ueda T (1985) Characterization of glutamate uptake into synaptic vesicles. *J Neurochem* 44(1):99-109.

53. Xu J, *et al.* (2008) GTP-independent rapid and slow endocytosis at a central synapse. *Nat Neurosci* 11(1):45-53.

54. Smith SM, Renden R, & von Gersdorff H (2008) Synaptic vesicle endocytosis: fast and slow modes of membrane retrieval. *Trends Neurosci* 31(11):559-568.

55. Huss M, *et al.* (2002) Concanamycin A, the specific inhibitor of V-ATPases, binds to the V(o) subunit c. *J Biol Chem* 277(43):40544-40548.

56. Macia E, *et al.* (2006) Dynasore, a cell-permeable inhibitor of dynamin. *Dev Cell* 10(6):839-850.

57. Lujan B, Kushmerick C, Banerjee TD, Dagda RK, & Renden R (2016) Glycolysis selectively shapes the presynaptic action potential waveform. *J Neurophysiol* 116(6):2523-2540.

58. Sobieski C, Warikoo N, Shu HJ, & Mennerick S (2018) Ambient but not local lactate underlies neuronal tolerance to prolonged glucose deprivation. *PLoS One* 13(4):e0195520.

59. Zilberter Y, Zilberter T, & Bregestovski P (2010) Neuronal activity in vitro and the in vivo reality: the role of energy homeostasis. *Trends Pharmacol Sci* 31(9):394-401.

60. Stryer L, Berg JM, & Tymoczko JL (2002) *Biochemistry (5th ed.)* (New York: W.H. Freeman).

61. Tsodyks MV & Markram H (1997) The neural code between neocortical pyramidal neurons depends on neurotransmitter release probability. *Proc Natl Acad Sci U S A* 94(2):719-723.

62. Cox DW & Bachelard HS (1982) Attenuation of evoked field potentials from dentate granule cells by low glucose, pyruvate + malate, and sodium fluoride. *Brain Res* 239(2):527-534.

63. Cox DW, Morris PG, Feeney J, & Bachelard HS (1983) 31P-n.m.r. studies on cerebral energy metabolism under conditions of hypoglycaemia and hypoxia in vitro. *Biochem J* 212(2):365-370.

64. Fleck MW, Henze DA, Barrionuevo G, & Palmer AM (1993) Aspartate and glutamate mediate excitatory synaptic transmission in area CA1 of the hippocampus. *J Neurosci* 13(9):3944-3955.

65. Kanatani T, Mizuno K, & Okada Y (1995) Effects of glycolytic metabolites on preservation of high energy phosphate level and synaptic transmission in the granule cells of guinea pig hippocampal slices. *Experientia* 51(3):213-216.

66. Pathak D, *et al.* (2015) The role of mitochondrially derived ATP in synaptic vesicle recycling. *J Biol Chem* 290(37):22325-22336.

67. Ma Y, *et al.* (2016) Resting-state hemodynamics are spatiotemporally coupled to synchronized and symmetric neural activity in excitatory neurons. *Proc Natl Acad Sci U S A* 113(52):E8463-E8471.

68. Wang Z, Wei X-X, Stocker AA, & Lee DD (2016) Efficient neural codes under metabolic constraints. *Advances in Neural Information Processing Systems*:4619-4627.

69. Ghavami S, Rahmati V, Lahouti F, & Schwabe L (2015) Synchrony in neuronal communication: An energy efficient scheme. *2015 Iran Workshop on Communication and Information Theory (IWCIT)*:1-6.

70. Ghavami S, Rahmati V, Lahouti F, & Schwabe L (2018) Neuronal Synchronization Can Control the Energy Efficiency of Inter-Spike Interval Coding. (arxiv: 1804.10090).

71. McCarthy KD & de Vellis J (1980) Preparation of separate astroglial and oligodendroglial cell cultures from rat cerebral tissue. *J Cell Biol* 85(3):890-902.

72. Syed YA, *et al.* (2008) Inhibition of oligodendrocyte precursor cell differentiation by myelin-associated proteins. *Neurosurg Focus* 24(3-4):E5.